

## Approach to ideal-gas behavior in dense classical fluids

Wouter Montfrooij

*Instituut Lorentz, Rijksuniversiteit Leiden, NL-2311 SB Leiden, The Netherlands*

Peter Verkerk and Ignatz de Schepper

*Interuniversitair Reactor Instituut, NL-2629 JB Delft, The Netherlands*

(Received 15 July 1985)

For a classical fluid of hard spheres we calculate for large wave numbers the leading correction to the ideal-gas behavior of the incoherent dynamic structure factor. The theoretical prediction agrees with results from neutron scattering experiments on dense hydrogen and sodium.

### I. INTRODUCTION

For a classical fluid of hard spheres in equilibrium the behavior of the incoherent dynamic structure factor  $S(k, \omega)$  as a function of frequency  $\omega$  and for large wave numbers  $k$  has been considered before by Sears.<sup>1,2</sup> He has found that the half-width at half maximum  $\omega_H(k)$  of  $S(k, \omega)$  is given, for large  $k$ , by

$$\omega_H(k) = (2k_B T m^{-1} \ln 2)^{1/2} k \left[ 1 - \frac{\xi}{k l_E} + O(k^{-2}) \right], \quad (1)$$

where  $k_B$  is the Boltzmann's constant,  $T$  the temperature,  $m$  the mass of the particles,  $l_E$  the (Enskog) mean free path between collisions, and  $\xi$  is estimated to be given by  $\xi \approx 0.27$ . The leading term on the right-hand side of Eq. (1) is due to the free motion of the particles, i.e., to ideal gas behavior, and the second term is due to one collision events between the hard spheres. Sears also has shown that the correction to the ideal gas behavior of  $\omega_H(k)$  of relative order  $k^{-1}$  [cf. Eq. (1)] is typical for hard spheres, since it is absent for systems of particles interacting through a soft potential. Using a value for the equivalent hard-sphere diameter  $\sigma_{HS}(T)$  of hydrogen molecules, taken from independent sources, he finds that the  $\omega_H(k)$  derived from neutron scattering experiments on hydrogen gas at  $T=85$  K and pressures  $p=35, 70,$  and  $140$  bars,<sup>3</sup> agree for large  $k$  with the hard-sphere result for  $\omega_H(k)$  given by Eq. (1). Recently, Morkel and Gläser<sup>4,5</sup> found from neutron scattering experiments on liquid sodium that the  $\omega_H(k)$  at  $602$  and  $803$  K and at saturated vapor pressures also agree with the hard-sphere  $\omega_H(k)$  for large  $k$  if  $\sigma_{HS}(T)$  (i.e.,  $l_E$ ) is used in Eq. (1) as an adjustable parameter. They obtain effective hard-sphere potentials which are realistic representations of the actual interparticle potential for sodium. Thus it appears that for large  $k$ , the behavior of  $\omega_H(k)$  for hydrogen and sodium can be described by that of the  $\omega_H(k)$  for equivalent hard-sphere fluids.

In this paper we calculate for hard spheres the leading correction of  $S(k, \omega)$  itself, to its ideal gas behavior. We base ourselves on the approach discussed before<sup>6</sup> for the intermediate incoherent scattering function  $F(k, t) = \int_{-\infty}^{+\infty} d\omega \exp(i\omega t) S(k, \omega)$  at large  $k$ . We rederive Eq. (1) for  $\omega_H(k)$  and give an exact expression for  $\xi$ . We also

derive a new expression, of the form of Eq. (1), for the maximum value  $S(k, 0)$  of  $S(k, \omega)$ , for large values of  $k$ .

Since the exact value of  $\xi$  (i.e.,  $\xi=0.4486$ ) is considerably different from the value estimated by Sears, we reconsider the experimental  $\omega_H$  results for  $H_2$  (cf. Ref. 2) and Na (cf. Ref. 4) in order to establish whether again the  $\omega_H$  for  $H_2$  and Na show a hard-sphere-like behavior. In addition we wish to determine in how far a hard-sphere-like behavior is also present in the top value  $S(k, 0)$  at large  $k$ . Therefore we use the experimental data for  $S(k, 0)$  given by Morkel and Gläser for Na.<sup>5</sup> For  $H_2$  we use data from a neutron scattering experiment performed at our Institute in Delft at  $T=300$  K and  $p=782$  bars in order to see whether not only  $\omega_H(k)$  but also  $S(k, 0)$  is hard-sphere-like. In Sec. II we review the theory and in Sec. III we compare the theory with experimental results. We conclude with a discussion in Sec. IV.

### II. THEORY

In this section we determine for a system of  $N$  hard spheres in equilibrium the leading corrections to ideal gas behavior for  $F(k, t)$  and  $S(k, \omega)$ . We start with  $F(k, t)$  which is defined for  $t > 0$  by<sup>6</sup>

$$F(k, t) = \langle e^{i\mathbf{k} \cdot \mathbf{r}_1} e^{iL t} e^{-i\mathbf{k} \cdot \mathbf{r}_1} \rangle, \quad (2)$$

where the brackets denote the canonical ensemble average,  $k = |\mathbf{k}|$  and  $L$  the (pseudo) Liouville operator for hard spheres

$$L = L_0 + \sum_{\substack{i, j=1 \\ i < j}}^N T(i, j), \quad (3)$$

with

$$L_0 = \sum_{i=1}^N \mathbf{v}_i \cdot \frac{\partial}{\partial \mathbf{r}_i}, \quad (4)$$

where  $\mathbf{v}_i$  and  $\mathbf{r}_i$  denote the velocity and position of particle  $i$  at  $t=0$ , respectively. In Eq. (3),  $L_0$  is due to free streaming and  $T(i, j)$  to a collision between particles  $i$  and  $j$ , i.e.,

$$T(i, j) = \sigma^2 \int d\hat{\sigma} |\mathbf{v}_{ij} \cdot \hat{\sigma}| \Theta(\mathbf{v}_{ij} \cdot \hat{\sigma}) \delta(\mathbf{r}_{ij} + \sigma \hat{\sigma}) [b_{\hat{\sigma}}(i, j) - 1], \quad (5)$$

where  $\sigma$  is the diameter of the hard spheres,  $\hat{\sigma}$  a unit vector characterizing a binary collision,  $\Theta(x)$  the unit step function and the substitution operator  $b_{\hat{\sigma}}(i,j)$  acts only on  $\mathbf{v}_i$  and  $\mathbf{v}_j$  and replaces them by the velocities after a binary collision, i.e.,

$$b_{\hat{\sigma}}(i,j)\mathbf{v}_i = \mathbf{v}_i - \hat{\sigma}(\hat{\sigma} \cdot \mathbf{v}_{ij}) ; \quad (6)$$

$$b_{\hat{\sigma}}(i,j)\mathbf{v}_j = \mathbf{v}_j + \hat{\sigma}(\hat{\sigma} \cdot \mathbf{v}_{ij}) .$$

We will need the expansion

$$e^{(A+B)t} = e^{At} + \int_0^t dt_1 e^{At_1} B e^{A(t-t_1)} + \int_0^t dt_1 \int_0^{t_1} dt_2 e^{At_2} B e^{A(t_1-t_2)} B e^{A(t-t_1)} + \dots , \quad (7)$$

useful for noncommuting operators  $A$  and  $B$ . With  $A=L_0$  and  $B=\sum_{i,j} T(i,j)$ , Eq. (7) is equivalent to the binary collision expansion in which the dynamics of the entire  $N$ -body hard-sphere fluid is expressed systematically in terms of contributions of zero, one, and two hard-sphere collisions. Using this result in Eq. (2) yields for the zero and one collision contribution to  $F(k,t)$ ,

$$F(k,t) = \langle e^{i\mathbf{k} \cdot \mathbf{r}_1} e^{tL_0} e^{-i\mathbf{k} \cdot \mathbf{r}_1} \rangle + \sum_{i,j} \int_0^t dt_1 \langle e^{i\mathbf{k} \cdot \mathbf{r}_1} e^{t_1 L_0} T(i,j) e^{(t-t_1)L_0} e^{-i\mathbf{k} \cdot \mathbf{r}_1} \rangle + \dots . \quad (8)$$

If we let the free streaming operators  $\exp(tL_0)$  act on  $\mathbf{r}_1$  and use  $T(i,j)f=0$  when  $f$  does not depend on  $\mathbf{v}_i$  and  $\mathbf{v}_j$  [cf. Eq. (5)], we find

$$F(k,t) = \langle e^{-i\mathbf{k} \cdot \mathbf{v}_1 t} \rangle + (N-1) \int_0^t dt_1 \langle e^{-i\mathbf{k} \cdot \mathbf{v}_1 t_1} T(1,2) e^{-i\mathbf{k} \cdot \mathbf{v}_1 (t-t_1)} \rangle + \dots . \quad (9)$$

In the following we shall use a time scale

$$\tau_k = (\beta m)^{1/2} / k \quad (10)$$

which is a time a particle needs to traverse the wavelength  $2\pi/k$  with thermal speed  $(\beta m)^{-1/2}$  (with  $\beta=1/k_B T$ ) as well as a reduced dimensionless time  $\tau$  and reduced velocities  $\mathbf{c}_j$  given by

$$\tau = t / \tau_k ,$$

$$\mathbf{c}_j = (\beta m)^{1/2} \mathbf{v}_j \quad (j=1,2,\dots,N) . \quad (11)$$

Then Eq. (9) reads, after evaluation of the zero collision (i.e., ideal gas) contribution,

$$F(k,t) = e^{-\tau^2/2} + \frac{(\beta m)^{1/2}(N-1)}{k} \int_0^\tau d\tau' \langle e^{-i\hat{\mathbf{k}} \cdot \mathbf{c}_1 \tau'} T(1,2) e^{-i\hat{\mathbf{k}} \cdot \mathbf{c}_1 (\tau-\tau')} \rangle + O(f_2(\tau)/k^2) , \quad (12)$$

where  $\hat{\mathbf{k}}=\mathbf{k}/k$  and the estimate  $k^{-2}f_2(\tau)$  for the two-collision contribution follows from the third term on the right-hand side of Eq. (7) and Eqs. (10) and (11). Thus we find that up to order  $k^{-2}$  the binary collision expansion leads to an expansion of  $F(k,t)$  in powers of  $1/k$  with coefficients which are functions of  $\tau$ . The one collision contribution in Eq. (12) is further evaluated in the Appendix with the result for  $t \geq 0$ ,

$$F(k,t) = e^{-\tau^2/2} + \frac{f_1(\tau)}{kl_E} + O(f_2(\tau)/k^2) \quad (13)$$

with

$$l_E = 1 / [\sqrt{2} \pi n \sigma^2 g(\sigma)] , \quad (14)$$

$n$  the number density,  $g(\sigma)$  the pair correlation function  $g(r)$  at contact, and

$$f_1(\tau) = \frac{2}{9} \left[ \frac{2}{\pi} \right]^{1/2} \tau^3 e^{-\tau^2/2} {}_2F_2\left(\frac{1}{2}, \frac{3}{2}; \frac{5}{2}, \frac{5}{2}; \frac{1}{4} \tau^2\right) , \quad (15)$$

where  ${}_2F_2$  is one of the generalized hypergeometric functions  ${}_pF_q$  defined in the Appendix. The result for  $F(k,t)$  given by Eqs. (13) and (15) is consistent with the result

given by Eq. (8.4) of Ref. 6 in which  $F(k,t)$  is expanded in powers of  $t/t_E$  with coefficients which are functions of  $\tau$ . Here  $t_E = (\pi \beta m / 8)^{1/2} l_E$  is the mean free time between collisions.

For the incoherent scattering function

$$S(k,\omega) = (2\pi)^{-1} \int_{-\infty}^{+\infty} dt \exp(-i\omega t) F(k,t)$$

we use  $F(k,-t) = F(k,t)$  so that

$$S(k,\omega) = \frac{1}{\pi} \int_0^\infty dt \cos(\omega t) F(k,t) . \quad (16)$$

Substitution of Eq. (13) for  $F(k,t)$  yields

$$S(k,\omega) = \left[ \frac{\beta m}{2\pi} \right]^{1/2} \frac{1}{k} \left[ e^{-(\omega^*)^2/2} + \frac{s_1(\omega^*)}{kl_E} + O(s_2(\omega^*)/k^2) \right] , \quad (17)$$

where the reduced dimensionless frequency  $\omega^*$  is given by

$$\omega^* = \omega \tau_k = \omega (\beta m)^{1/2} / k \quad (18)$$

and where

$$s_1(\omega^*) = \frac{4}{9\pi} \int_0^\infty d\tau \cos(\omega^* \tau) e^{-\tau^2/2\tau^3} \times {}_2F_2\left(\frac{1}{2}, \frac{3}{2}; \frac{5}{2}, \frac{5}{2}; \frac{1}{4}\tau^2\right). \quad (19)$$

Thus,  $S(k, \omega)$  is expressed as a series in  $1/k$  in which the coefficients are functions of the reduced frequency  $\omega^*$ , the leading term being the ideal gas contribution. From the expansion of  $\cos(\omega^* \tau)$  in powers of  $\omega^* \tau$  it follows that [cf. Eq. (19)],

$$s_1(\omega^*) = \frac{8}{9\pi} \sum_{j=0}^{\infty} \frac{(j+1)!}{(2j)!} {}_3F_2\left(\frac{1}{2}, \frac{3}{2}, j+2; \frac{5}{2}, \frac{5}{2}; \frac{1}{2}\right) \times [-2(\omega^*)^2]^j, \quad (20)$$

which series converges absolutely for all  $\omega^*$ . We have calculated  $s_1(\omega^*) = s_1(-\omega^*)$  numerically for  $0 \leq \omega^* \leq 5$  using a few hundred terms in the expansion on the right-hand side of Eq. (20), thereby verifying the convergence of the results. We show  $s_1(\omega^*)$  in Fig. 1. We observe that  $s_1(\omega^*)$  is positive for  $0 \leq \omega^* \leq 0.81$ , negative for  $0.81 \leq \omega^* \leq 2.66$ , and positive again for  $\omega^* \geq 2.66$ . For large  $\omega^*$ ,  $s_1(\omega^*)$  behaves as [cf. Eq. (19)]

$$s_1(\omega^*) = \frac{8}{3\pi(\omega^*)^4} + O(1/(\omega^*)^6), \quad (21)$$

and therefore decays very slowly  $\sim (\omega^*)^{-4}$  compared to the leading ideal gas contribution  $\sim \exp[-(\omega^*)^2/2]$  in Eq. (17). Thus, for a fixed but large value of  $kl_E$  the second term in the expansion of  $S(k, \omega)$  on the right-hand side of Eq. (17) increasingly exceeds the first term when  $\omega^*$  increases. However, since for all  $k$  and large  $\omega$ ,

$$S(k, \omega) = \frac{2k^2}{3\pi\beta m t_E} \frac{1}{\omega^4} + O(1/\omega^6), \quad (22)$$

the behavior of  $s_1(\omega^*)$  for large  $\omega^*$  yields the exact behavior of  $S(k, \omega)$  so that Eq. (17) still applies when  $\omega^* \rightarrow \infty$ . The contributions of the free streaming and of the terms of relative order  $k^{-2}$  and higher are irrelevant then.

Next we consider the maximum value  $S(k, 0)$  and the half-width  $\omega_H(k)$  of  $S(k, \omega)$ . From Eqs. (17) and (20) it follows that

$$S(k, 0) = \left[ \frac{\beta m}{2\pi} \right]^{1/2} \frac{1}{k} \left[ 1 + \frac{s_1(0)}{kl_E} + O(1/k^2) \right], \quad (23)$$

where

$$s_1(0) = \frac{8}{9\pi} {}_3F_2\left(\frac{1}{2}, \frac{3}{2}, 2; \frac{5}{2}, \frac{5}{2}; \frac{1}{2}\right) = 0.32808. \quad (24)$$

Thus, the leading hard-sphere correction to  $S(k, 0)$  is of relative order  $1/k$ , similar to  $\omega_H(k)$  [cf. Eq. (1)]. The half-width  $\omega_H(k)$  is defined by  $S(k, \omega_H(k)) = \frac{1}{2} S(k, 0)$  so that [cf. Eq. (17)]

$$\omega_H(k) = \left[ \frac{2 \ln 2}{\beta m} \right]^{1/2} k \left[ 1 - \frac{\xi}{kl_E} + O(1/k^2) \right], \quad (25)$$

with

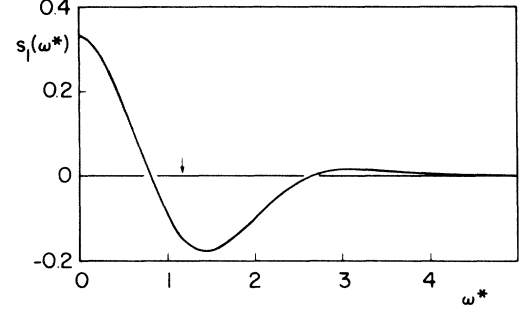


FIG. 1. The first correction  $s_1(\omega^*)$  to the ideal gas  $S(k, \omega)$  for a hard-sphere fluid [cf. Eq. (17)] as a function of  $\omega^* = (\beta m)^{1/2} \omega / k$ . The arrow points to the value of  $\omega^*$  where the ideal gas  $S(k, \omega)$  has its half-width at half maximum.

$$\xi = \frac{s_1(0) - 2s_1(\sqrt{2 \ln 2})}{2 \ln 2} = 0.4486. \quad (26)$$

Thus we recover Eq. (1), including an exact expression for  $\xi$ .

We note that the zeroth and second moments of  $s_1(\omega^*)$  vanish, i.e.,

$$\int_{-\infty}^{+\infty} d\omega^* s_1(\omega^*) = \int_{-\infty}^{+\infty} d\omega^* (\omega^*)^2 s_1(\omega^*) = 0$$

since

$$\int_{-\infty}^{+\infty} d\omega^* \exp(i\omega^* \tau) s_1(\omega^*) = (2\pi)^{1/2} f_1(\tau)$$

[cf. Eq. (16)] and since  $f_1(0) = 0$  and  $\partial^2 f_1(\tau) / \partial \tau^2 = 0$  for  $\tau = 0$ . Therefore the zeroth and second moments of  $S(k, \omega)$  are not affected by the leading hard-sphere correction term in Eq. (17) and are given by the ideal gas values 1 and  $k^2/\beta m$ , respectively, which are exact for all  $k$ . Since  $s_1(0) > 0$ , the leading hard-sphere correction to  $S(k, 0)$  from ideal gas behavior is positive [cf. Eq. (23)]. Since  $s_1(\omega^*) < 0$  for the reduced ideal gas half-width  $\omega^* = (2 \ln 2)^{1/2}$  (cf. Fig. 1), the leading hard-sphere correction to the ideal gas  $\omega_H(k)$  is negative [cf. Eq. (25)]. Thus, the spectra  $S(k, \omega)$  with the leading hard-sphere correction included are sharper than the corresponding ideal gas spectra and show a tail  $\sim \omega^{-4}$  for large  $\omega$ , typical for hard spheres.

### III. EXPERIMENTS

In this section we compare the theoretical results for  $\omega_H(k)$  and  $S(k, 0)$  derived in the previous section for hard spheres with results obtained from neutron scattering experiments on hydrogen and sodium.

#### A. Hydrogen at 85 K

Sears has compared his theoretical prediction for  $\omega_H$  [cf. Eq. (1) with  $\xi = 0.27$ ] with the  $\omega_H$  obtained from neutron scattering experiments on hydrogen gas at  $T = 85$  K and  $p = 35, 70$  and  $140$  bars.<sup>2,3</sup> He uses an equivalent hard-sphere diameter  $\sigma_{HS}(T) = 2.91$  Å for the hydrogen molecules which is derived from the actual values of the coefficients of self-diffusion  $D$  at this temperature. In fact, Sears has compared (cf. Fig. 2) the experimentally

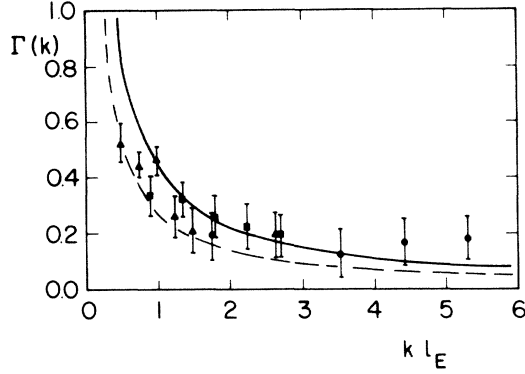


FIG. 2. The relative deviation  $\Gamma(k) = 1 - \omega_H/\omega_H^{\text{id}}$  of the half-width  $\omega_H$  from its ideal gas behavior  $\omega_H^{\text{id}}$  for hydrogen gas at 85 K and 35 bars (●), 70 bars (■), and 140 bars (▲) (cf. Ref. 2), as functions of  $kl_E$  where  $\sigma_{\text{HS}} = 2.91 \text{ \AA}$  and  $l_E$  is the corresponding mean free path. The curves are the asymptotic hard-sphere results  $\xi/(kl_E)$  with  $\xi = 0.27$  (---) (cf. Ref. 1) and with  $\xi = 0.45$  (—) [cf. Eq. (26)].

derived relative deviation  $\Gamma(k) = 1 - \omega_H/\omega_H^{\text{id}}$  of  $\omega_H$  from its ideal gas behavior  $\omega_H^{\text{id}} = (2k_B T m^{-1} \ln 2)^{1/2} k$  for  $\text{H}_2$  with the theoretical hard-sphere prediction  $\Gamma(k) = \xi/(kl_E)$  [cf. Eqs. (1) and (25)]. We observe in Fig. 2 that the agreement between theory and experiment using the exact value  $\xi = 0.45$  is better for  $kl_E > 1$  than the agreement using the estimate  $\xi = 0.27$ . Therefore, Sears's conclusion that  $\omega_H$  of  $\text{H}_2$  shows a hard-sphere-like behavior for large  $k$  is strengthened when the exact value of  $\xi$  is used in Eq. (1) instead of his estimated value.

### B. Sodium at saturated vapor pressure

Morkel and Gläser<sup>4,5</sup> have compared their experimental neutron scattering results for  $\omega_H$  of liquid sodium at  $n = 0.0229 \text{ \AA}^{-3}$ ,  $T = 602 \text{ K}$  and  $n = 0.0216 \text{ \AA}^{-3}$ ,  $T = 803 \text{ K}$ , with the theoretical hard-sphere result [cf. Eq. (1)] with  $\xi = 0.27$ . For large  $k$  they find a very good agreement between theory and experiment when<sup>5</sup>  $l_E = 0.26 \text{ \AA}$  at 602 K and  $l_E = 0.37 \text{ \AA}$  at 803 K corresponding to equivalent hard-sphere diameters  $\sigma_{\text{HS}}(T) = 3.22 \text{ \AA}$  at 602 K and  $\sigma_{\text{HS}}(T) = 3.11 \text{ \AA}$  at 803 K. Here we compare the experimental data for  $\omega_H$  and  $S(k,0)$  with the exact asymptotic hard-sphere results [cf. Eq. (1) with  $\xi = 0.45$  and Eq. (25)]. In fact we consider, as in Refs. 4 and 5, the more convenient reduced quantities  $\omega_H/k^2$  and  $S(k,0)k^2$  since these tend to the constants  $D$  and  $(\pi D)^{-1}$ , respectively, for small  $k$ . The experimental results of Morkel and Gläser are displayed in Fig. 3 for  $\omega_H/k^2$  and in Fig. 4 for  $S(k,0)k^2$ . We find that both  $\omega_H/k^2$  and  $S(k,0)k^2$  show a hard-sphere-like behavior for  $kl_E > 1$  when we use the corrected values  $l_E^c = 0.43 \text{ \AA}$  and  $\sigma_{\text{HS}}^c(T) = 2.96 \text{ \AA}$  at 602 K [cf. Figs. 3(a) and 4(a)] and  $l_E^c = 0.61 \text{ \AA}$  and  $\sigma_{\text{HS}}^c(T) = 2.83 \text{ \AA}$  at 803 K [cf. Figs. 3(b) and 4(b)]. Thus not only is  $\omega_H$  hard-sphere-like, as Morkel and Gläser have concluded, but so is  $S(k,0)$ , as we find here. In the next paragraph we study both  $\omega_H$  and  $S(k,0)$  for  $\text{H}_2$ .

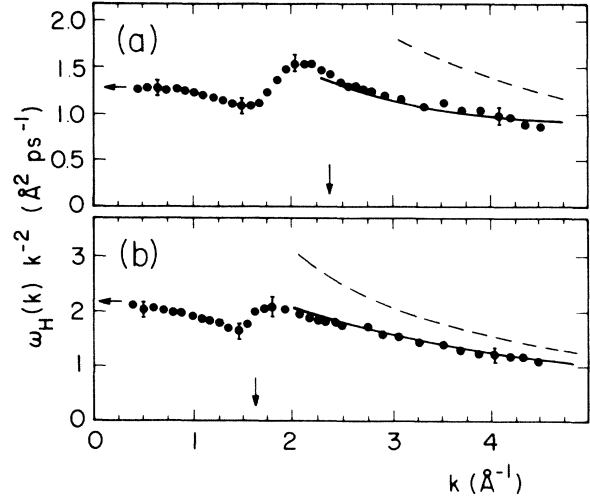


FIG. 3. The reduced half-widths  $\omega_H/k^2$  as functions of  $k$  for liquid sodium (●) (cf. Ref. 5) at saturated vapor pressure and 602 K (a) and 803 K (b), for the corresponding ideal gas fluids (---) and for hard spheres (—) with  $\xi = 0.45$ ,  $\sigma_{\text{HS}} = 2.96 \text{ \AA}$ ,  $l_E = 0.33 \text{ \AA}$  (a) and  $\sigma_{\text{HS}} = 2.83 \text{ \AA}$ ,  $l_E = 0.61 \text{ \AA}$  (b). The vertical arrows point to where  $kl_E = 1$ , the horizontal arrows to where  $\omega_H/k^2 = D$ , with  $D$  the coefficient of self-diffusion of sodium.

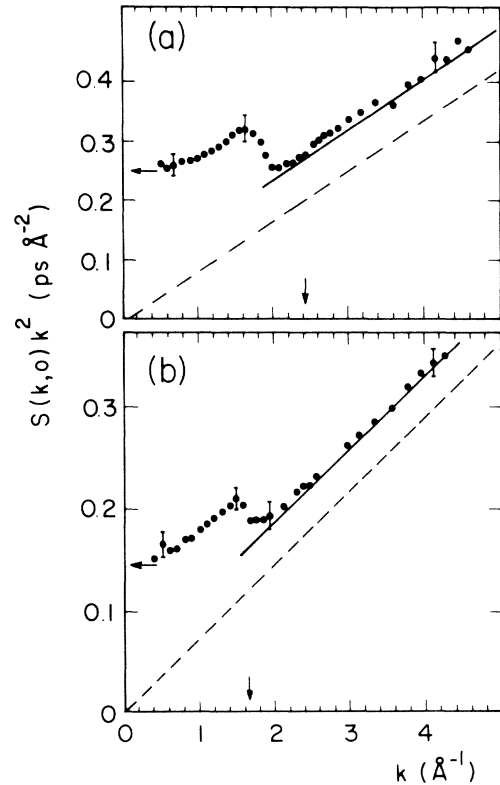


FIG. 4. The reduced top values  $S(k,0)k^2$  as functions of  $k$  for liquid sodium (●) (cf. Ref. 5) at 602 K (a) and 803 K (b), for the corresponding ideal gas fluids (---) and for hard spheres (—) with  $\sigma_{\text{HS}} = 2.96 \text{ \AA}$  (a) and  $\sigma_{\text{HS}} = 2.83 \text{ \AA}$  (b). The vertical arrows point to where  $kl_E = 1$ , the horizontal arrows point to where  $S(k,0)k^2 = (\pi D)^{-1}$ .

## C. Hydrogen at 300 K

We have performed a neutron scattering experiment on hydrogen gas at  $T=300$  K,  $n=0.0129$  Å<sup>-3</sup> and  $p=782$  bars. We use the RKS-1 rotating crystal time-of-flight spectrometer at the Delft 2 MW light-water swimming-pool reactor. The wavelength of the incoming neutrons was 4 Å. The sample container and the correction procedures used to obtain the incoherent  $S(k,\omega)$  from the measured neutron intensities are described in Ref. 7. The experimental results for  $\omega_H(k)/k^2$  and  $S(k,0)k^2$  are displayed in Fig. 5. In order to compare our results with the exact theoretical hard-sphere predictions we use for H<sub>2</sub> the equivalent hard-sphere diameter  $\sigma_{HS}(T)=2.56$  Å. This value of  $\sigma_{HS}$  has been derived by Chen *et al.*<sup>8</sup> from low-density diffusion data for H<sub>2</sub> at  $T=300$  K. The theoretical predictions for  $\omega_H$  and  $S(k,0)$  with  $l_E=1.94$  Å are shown in Fig. 5. We observe in Fig. 5(a) that for  $kl_E > 1$  the experimental values of  $\omega_H(k)/k^2$  approach the corresponding ideal gas behavior in a hard-sphere-like manner. In addition, for  $kl_E > 1$ , the deviations of the experimental  $S(k,0)k^2$  from ideal gas behavior follow the prediction calculated for a hard-sphere fluid [cf. Fig. 5(b)]. Therefore, for hydrogen, not only  $\omega_H(k)$  is hard-sphere-like for large  $k$ , but also  $S(k,0)$ . In Fig. 5 we also show the  $k=0$  limits of  $\omega_H(k)/k^2$  and  $S(k,0)k^2$ , i.e.,  $D$  and  $(\pi D)^{-1}$ , respectively, with  $D=23.8$  Å<sup>2</sup>/ps. We estimated this value of  $D$  from an extrapolation of results

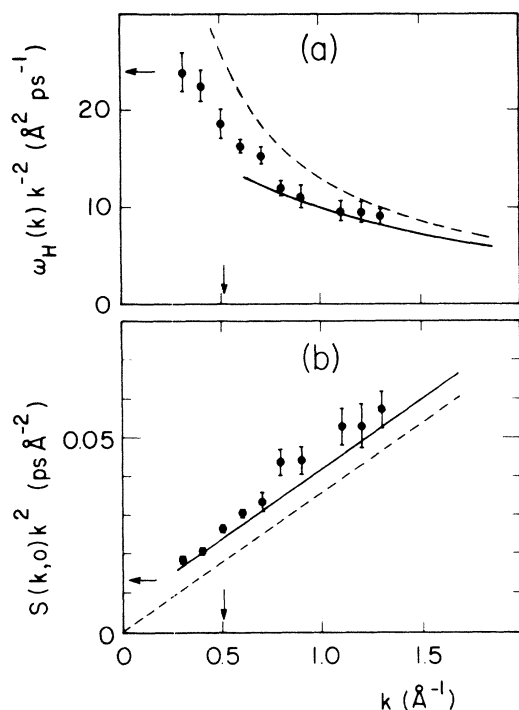


FIG. 5. The reduced half-widths  $\omega_H/k^2$  (a) and top values  $S(k,0)k^2$  (b) as functions of  $k$  for hydrogen gas (●) at 300 K and 782 bars, for the corresponding ideal gas fluid (---) and for hard spheres (—) with  $\sigma_{HS}=2.56$  Å and  $l_E=1.94$  Å. The vertical arrow points to where  $kl_E=1$ . The horizontal arrows point to where  $\omega_H/k^2=D$  (a) and  $S(k,0)k^2=(\pi D)^{-1}$  (b) with  $D=23.8$  Å<sup>2</sup>/ps.

for  $D$  obtained by Chen *et al.*<sup>8</sup> from small  $k$  neutron scattering data at 300 K at three densities neighboring to the present one. We note that the value  $D=23.8$  Å<sup>2</sup>/ps is close to the diffusion coefficient  $D_{HS}=23$  Å<sup>2</sup>/ps of the equivalent hard-sphere fluid.<sup>8-10</sup> Although our experiment was performed with little emphasis on small  $k$  values we still observe in Fig. 5 that the experimental  $\omega_H(k)$  and  $S(k,0)$  show a tendency towards the corresponding small  $k$  limits.

## IV. DISCUSSION

Using temperature-dependent hard-sphere diameters  $\sigma_{HS}(T)$  for H<sub>2</sub> and Na particles we find that the half-width  $\omega_H(k)$  of  $S(k,\omega)$  for H<sub>2</sub> at 85 K and the  $\omega_H(k)$  and  $S(k,0)$  for H<sub>2</sub> at 300 K and Na at 602 K and 803 K approach for  $kl_E > 1$  the corresponding ideal gas limits in a hard-sphere-like manner. In order to assess the physical significance of the  $\sigma_{HS}(T)$  used in our comparisons, we show the Silvera-Goldman potential<sup>11</sup> for H<sub>2</sub> in Fig. 6(a) and the Rasolt-Taylor potential<sup>12</sup> for Na in Fig. 6(b). In addition we display our effective hard-sphere potentials for H<sub>2</sub> with  $\sigma_{HS}(T)=2.91$  Å at 85 K and 2.56 Å at 300 K in Fig. 6(a) and for Na with  $\sigma_{HS}(T)=2.96$  Å at 602 K and 2.83 Å at 803 K in Fig. 6(b). We observe in Fig. 6 that our effective hard-sphere potentials are model potentials representative for the repulsive parts of the actual interparticle interaction  $\Phi(r)$  both for H<sub>2</sub> and Na and that the decrease of  $\sigma_{HS}(T)$  with increasing temperature  $T$  is a reflection of the softness of the repulsive parts of  $\Phi(r)$  for H<sub>2</sub> and Na. Also, we note that the apparent insignificance of the attractive parts of  $\Phi(r)$  for the experimental

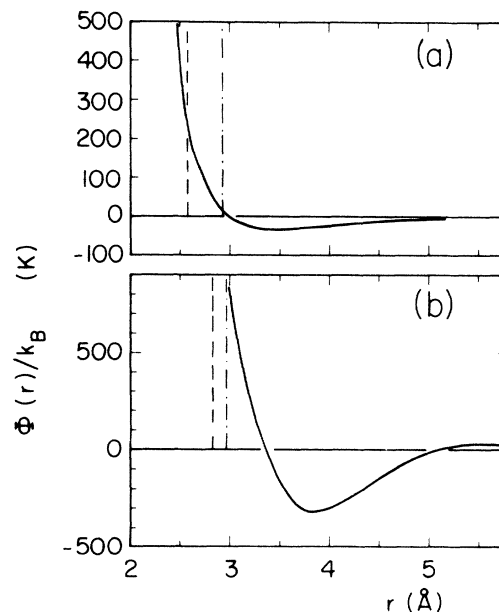


FIG. 6. The reduced potentials  $\Phi(r)/k_B$  for H<sub>2</sub> (cf. Ref. 11) [solid curve in (a)] and Na (cf. Ref. 12) [solid curve in (b)] as functions of the interparticle separation  $r$ . Also shown are the equivalent hard-sphere potentials for H<sub>2</sub> at 85 K [--- in (a)], and 300 K [--- in (a)] and for Na at 602 K [--- in (b)] and 803 K [--- in (b)].

$\omega_H(k)$  and  $S(k,0)$  considered in this paper might be due to the fact that thermodynamic states are studied for which the average kinetic energy  $k_B T$  of the particles is large compared to the well depth  $\epsilon$  of  $\Phi(r)$  (cf. Fig. 6).

Recently van Well and de Graaf<sup>13</sup> studied the results for the coherent scattering function obtained from neutron scattering experiments on liquid Ar at 120 K. For large  $k$  they find that the approach to ideal gas behavior in Ar is the same as that observed in a corresponding Lennard-Jones (LJ) fluid<sup>14</sup> with  $\sigma_{LJ}=3.36$  Å and  $\epsilon/k_B=123$  K, but that both approaches differ significantly for  $kl_E > 1$  from that in a corresponding hard-sphere fluid with  $\sigma_{HS}=3.43$  Å. For dense fluids it seems therefore that while the approach to ideal gas behavior is hard-sphere-like for  $kl_E > 1$  and  $k_B T > \epsilon$ , such a behavior is absent for  $kl_E > 1$  when  $k_B T \lesssim \epsilon$ . Probably, the influence of the attractive part of the interaction potential on  $S(k,\omega)$  extends up to very large values of  $k$  then. This conclusion is further supported by recent comparisons of molecular dynamics (MD) simulation results for Lennard-Jones (LJ) fluids and kinetic theory calculations

for hard spheres at intermediate values of  $k$ . At  $k_B T/\epsilon=1.47$ , Ullo and Yip<sup>15</sup> find no differences in the half-width  $\omega_H^c(k)$  of the coherent scattering function when  $6 \lesssim k\sigma_{LJ} \lesssim 10$  for LJ fluids, the corresponding results of neutron scattering experiments on krypton<sup>16</sup> and the theoretical hard-sphere values. Therefore they conclude that at  $k_B T/\epsilon=1.47$  and intermediate  $k$  values, the details of the potential are irrelevant and the fluids behave hard-sphere-like, similar as we find here for Na and H<sub>2</sub> at large  $k$ . A similar comparison<sup>17</sup> at  $k_B T/\epsilon=0.97$  and  $6 \lesssim k\sigma_{LJ} \lesssim 12$  shows that the  $\omega_H^c(k)$  of LJ systems<sup>14</sup> agree with those of corresponding argon fluids<sup>18</sup> but differ considerably from the theoretical hard-sphere results. Thus at  $k_B T/\epsilon=0.97$ , LJ fluids do not behave hard-sphere-like at intermediate values of  $k$  and the details of the potential are still relevant then, as they are at large  $k$  (cf. Ref. 13).

#### ACKNOWLEDGMENTS

One of us (I.d.S.) gratefully acknowledges the useful discussions with M. J. Zuilhof and E. G. D. Cohen.

#### APPENDIX

Here we evaluate the function  $f_1(\tau)$  defined by the Eqs. (12) and (13), i.e.,

$$f_1(\tau) = (\beta m)^{1/2} l_E (N-1) \int_0^\tau d\tau' \langle e^{-i\hat{\mathbf{k}} \cdot \mathbf{c}_1 \tau'} T(1,2) e^{-i\hat{\mathbf{k}} \cdot \mathbf{c}_1 (\tau - \tau')} \rangle. \quad (\text{A1})$$

From Eq. (5) for  $T(i,j)$ , the definition of  $g(r)$  (Ref. 6) and Eq. (14) for  $l_E$  follows straightforwardly that

$$f_1(\tau) = \frac{1}{\sqrt{2\pi}} \int_0^\tau d\tau' \int d\hat{\sigma} \langle \langle e^{-i\hat{\mathbf{k}} \cdot \mathbf{c}_1 \tau'} | \mathbf{c}_{12} \cdot \hat{\sigma} | \Theta(\mathbf{c}_{12} \cdot \hat{\sigma}) [b_{\hat{\sigma}}(1,2) - 1] e^{-i\hat{\mathbf{k}} \cdot \mathbf{c}_1 (\tau - \tau')} \rangle \rangle_{12}, \quad (\text{A2})$$

where the two sets of labeled angle brackets refer to the reduced normalized velocity averages

$$\langle (\dots) \rangle_j = (2\pi)^{-3/2} \int d\mathbf{c}_j e^{-c_j^2/2} (\dots). \quad (\text{A3})$$

In Eq. (A2) we replace  $\Theta(\mathbf{c}_{12} \cdot \hat{\sigma})$  by  $\frac{1}{2}$ , since  $b_{\hat{\sigma}} = b_{-\hat{\sigma}}$  [cf. Eq. (6)]. We use the reduced center-of-mass velocity  $\mathbf{C} = (\mathbf{c}_1 + \mathbf{c}_2)/2$  and the reduced relative velocity  $\mathbf{c} = \mathbf{c}_{12}$ . Since  $b_{\hat{\sigma}}$  in Eq. (A2) acts only the component of  $\mathbf{c}$  in the  $\hat{\sigma}$  direction, i.e., on  $c_\sigma = \mathbf{c} \cdot \hat{\sigma}$ , we may integrate over  $\mathbf{C}$  and over the two components of  $\mathbf{c}$  orthogonal to  $\hat{\sigma}$ . Then

$$f_1(\tau) = \frac{\sqrt{2}}{4\pi} e^{-\tau^2/2} \int_0^\tau d\tau' \int d\hat{\sigma} e^{(\hat{\mathbf{k}} \cdot \hat{\sigma})^2 \tau^2/4} \langle e^{-i\hat{\mathbf{k}} \cdot \hat{\sigma} c_\sigma \tau'/2} | c_\sigma | (b_{\hat{\sigma}} - 1) e^{-i\hat{\mathbf{k}} \cdot \hat{\sigma} c_\sigma (\tau - \tau')/2} \rangle_r, \quad (\text{A4})$$

with

$$\langle (\dots) \rangle_r = (4\pi)^{-1/2} \int_{-\infty}^{+\infty} dc_\sigma e^{-c_\sigma^2/4} (\dots). \quad (\text{A5})$$

We use  $b_{\hat{\sigma}} c_\sigma = -c_\sigma$  and perform the  $\tau'$  integral. Thus,

$$f_1(\tau) = \frac{\sqrt{2}}{4\pi} e^{-\tau^2/2} \int d\hat{\sigma} e^{(\hat{\mathbf{k}} \cdot \hat{\sigma})^2 \tau^2/4} \left\langle | c_\sigma | \left[ \frac{e^{i\hat{\mathbf{k}} \cdot \hat{\sigma} c_\sigma \tau/2}}{i\hat{\mathbf{k}} \cdot \hat{\sigma} c_\sigma/2} - \tau e^{i\hat{\mathbf{k}} \cdot \hat{\sigma} c_\sigma \tau/2} \right] \right\rangle_r, \quad (\text{A6})$$

or, more conveniently,

$$f_1(\tau) = -\frac{\sqrt{2}}{8\pi} e^{-\tau^2/2} \int_0^\tau d\tau' \tau' \int d\hat{\sigma} i\hat{\mathbf{k}} \cdot \hat{\sigma} e^{(\hat{\mathbf{k}} \cdot \hat{\sigma})^2 \tau^2/4} \times \langle | c_\sigma | c_\sigma e^{i\hat{\mathbf{k}} \cdot \hat{\sigma} c_\sigma \tau'/2} \rangle_r. \quad (\text{A7})$$

In the following we need the hypergeometric functions  ${}_pF_q$  which are defined by<sup>19</sup>

$${}_pF_q(\alpha_1, \alpha_2, \dots, \alpha_p; \beta_1, \beta_2, \dots, \beta_q; z) = \sum_{n=0}^{\infty} \frac{(\alpha_1)_n (\alpha_2)_n \times \dots \times (\alpha_p)_n z^n}{(\beta_1)_n (\beta_2)_n \times \dots \times (\beta_q)_n n!}, \quad (\text{A8})$$

where

$$(\alpha)_n = \alpha(\alpha+1) \times \cdots \times (\alpha+n-1) = \frac{\Gamma(\alpha+n)}{\Gamma(\alpha)} \quad (\text{A9})$$

is a Pochhammer symbol and  $\Gamma(x)$  the gamma function.

In Eq. (A7) we expand  $\exp(i\hat{\mathbf{k}} \cdot \hat{\boldsymbol{\sigma}} c_\sigma \tau'/2)$ , use only the terms which are odd in  $\hat{\mathbf{k}} \cdot \hat{\boldsymbol{\sigma}}$ , and perform the average  $\langle (\cdots) \rangle_r$ , and the  $\tau'$  integral term by term. Then,

$$f_1(\tau) = \frac{\sqrt{2}}{6\pi^{3/2}} \tau^3 e^{-\tau^2/2} \int d\hat{\boldsymbol{\sigma}} (\hat{\mathbf{k}} \cdot \hat{\boldsymbol{\sigma}})^2 \times {}_1F_1\left(\frac{1}{2}; \frac{5}{2}; \frac{1}{4} (\hat{\mathbf{k}} \cdot \hat{\boldsymbol{\sigma}})^2 \tau^2\right), \quad (\text{A10})$$

where we used  ${}_1F_1(\alpha; \beta; z) = {}_1F_1(\beta - \alpha; \beta; -z) \exp z$ , for the confluent hypergeometric function  ${}_1F_1$ .<sup>20</sup>

In Eq. (A10) we expand  ${}_1F_1$  and perform the  $\hat{\boldsymbol{\sigma}}$  integral term by term, so that

$$f_1(\tau) = \frac{2\sqrt{2}}{9\sqrt{\pi}} \tau^3 e^{-\tau^2/2} {}_2F_2\left(\frac{1}{2}, \frac{3}{2}; \frac{5}{2}, \frac{5}{2}; \frac{1}{4} \tau^2\right), \quad (\text{A11})$$

which is the final result for  $f_1(\tau)$ .

<sup>1</sup>V. F. Sears, Phys. Rev. A 5, 452 (1972).

<sup>2</sup>V. F. Sears, Phys. Rev. A 7, 340 (1973).

<sup>3</sup>Y. Lefevre, S.-H. Chen, and S. Yip, *Neutron Inelastic Scattering* (IAEA, Vienna, 1972).

<sup>4</sup>W. Gläser and Ch. Morkel, J. Non-Cryst. Solids 61, 309 (1984).

<sup>5</sup>Ch. Morkel, Doctoral thesis, Technische Universität München, FRG, 1984 (unpublished).

<sup>6</sup>I. M. de Schepper, M. H. Ernst, E. G. D. Cohen, J. Stat. Phys. 25, 321 (1981).

<sup>7</sup>P. Verkerk, J. H. Builtjes, and I. M. de Schepper, Phys. Rev. A 31, 1731 (1985).

<sup>8</sup>S.-H. Chen, T. A. Postol, and K. Sköld, Phys. Rev. A 16, 2112 (1977).

<sup>9</sup>B. J. Alder, D. M. Gass, and T. E. Wainwright, J. Chem. Phys. 53, 3813 (1970).

<sup>10</sup>W. W. Wood, in *Fundamental Problems in Statistical Mechanics III*, edited by E. G. D. Cohen (North-Holland, Amsterdam, 1975).

<sup>11</sup>I. F. Silvera and V. V. Goldman, J. Chem. Phys. 69, 4209 (1978).

<sup>12</sup>M. Rasolt and R. Taylor, Phys. Rev. B 11, 2717 (1975).

<sup>13</sup>A. A. van Well and L. A. de Graaf, Phys. Rev. A 32, 2384 (1985).

<sup>14</sup>J. C. van Rijs and C. Bruin (unpublished).

<sup>15</sup>J. J. Ullo and S. Yip, Phys. Rev. A 29, 2092 (1984).

<sup>16</sup>P. A. Egelstaff, W. Gläser, D. Litchinsky, E. Schneider, and J.-B. Suck, Phys. Rev. A 27, 1106 (1982).

<sup>17</sup>I. M. de Schepper, E. G. D. Cohen, and M. J. Zuilhof, Phys. Lett. 101A, 399 (1984).

<sup>18</sup>A. A. van Well, P. Verkerk, L. A. de Graaf, J.-B. Suck, and J. R. D. Copley, Phys. Rev. A 31, 3391 (1985).

<sup>19</sup>I. S. Gradshteyn and I. W. Ryzhik, *Table of Integrals Series and Products* (Academic, New York, 1965).

<sup>20</sup>*Handbook of Mathematical Functions*, edited by M. Abramowitz and I. A. Stegun (Dover, New York, 1970).